Korean J. of Chem. Eng., 9(1), 8-15 (1992)

SIMULATION OF SILICON FILM GROWTH BY SILANE DECOMPOSITION AT LOW PRESSURES AND TEMPERATURES

Ju Hyung Lee, Sang Heup Moon* and Shi-Woo Rhee**

Dept. of Chem. Eng., Seoul National University, Kwanak-ku, Shinlim-dong, San 56-1, Seoul, Korea
**Dept. of Chem. Eng., Pohang Institute of Science and Technology, P.O. Box 125, Pohang, Korea
(Received 13 September 1991 • accepted 30 December 1991)

Abstract—Silicon film deposition by silane decomposition in LPCVD (Low Pressure Chemical Vapor Deposition) process has been simulated by numerical computation of the governing transport and reaction equations, assuming that the rate of silane decomposition in the gas phase controls the overall film growth rate. The film growth rate and the film uniformity increase with the reactant flow rate when the flow rate is relatively low, but they decrease at higher flow rates due to the negative effect of the reduced reaction time in the reactor. Accordingly, the film deposition process is optimized by controlling the reactant flow rate so that the position of the maximum SiH_4-decomposition rate in the gas phase is located above the substrate region. With a larger degree of the substrate tilting, the growth rate decreases but the film uniformity is improved. The film uniformity is also improved when the pressure is low.

INTRODUCTION

Epitaxial Si-film growth, one of the key processes in fabrication of bipolar device, is usually carried out by APCVD (Atmospheric Pressure Chemical Vapor Deposition) method. Since the process is carried out at high temperatures, above 1000℃, it is subject to drawbacks such as autodoping and solid-state diffusion. The drawbacks cause serious problems particularly in the modern ULSI devices that are fabricated to the line features of sub-micron level.

As an alternative to APCVD, LPCVD (Low Pressure CVD) processes carried out at medium vacuum (30-250 Pa, or 0.25-2 Torr) and moderate temperatures (550-600℃) have been developed [1]. Up to the present time, however, most of the efforts to analyze CVD processes theoretically have been concentrated on APCVD. In modeling of APCVD, it is usually assumed that the film growth rate is limited by the rate of reactant transfer to the surface rather than by reaction rate in the gas phase or on the substrate surface. This is because the reactant transfer rate is much slower than the reaction rate under the conditions of high temperature and atmospheric pressure.

However, as the pressure of the CVD process is lowered, the mass transfer is enhanced and becomes comparable to the reaction rates [2]. When SiH_4 is used as a reactant, the rate of SiH_4 decomposition in the gas phase plays an important role in determining the overall film growth rate [3, 4]. Following this view, Coltrin et al. [3, 4] have proposed a model to include many gas phase reactions in addition to the mass transfer step, but their works have been on APCVD processes.

In this work, we have simulated a SiH_4-LPCVD process based on a model which operates at low pressures and temperatures so that the overall film growth rate is controlled by the gas-phase reaction.

MODEL FORMULATION

Fig. 1 shows an idealized CVD reactor with a tilted susceptor, which has been considered as a model reactor in this study. The reactor operates at relatively low temperatures, $T_{wall}=500$℃ and $T_{susceptor}=800$℃, and the pressure is as low as 10 mTorr. Typical operating conditions of the reactor are shown in Table 1.

1. Transport Equations

A series of unit steps that could lead to film deposition in a CVD system include transport of gaseous species, chemical reactions in the gas phase, adsorption and reaction on the wafer surface. Accordingly, equations to describe the momentum, energy and

*To whom correspondence related to this paper should be addressed.

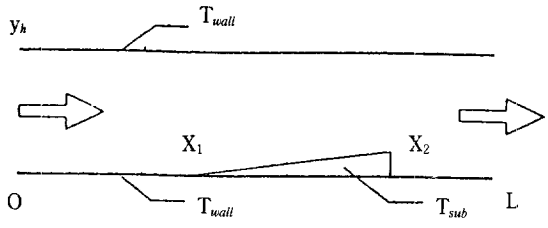

Fig. 1. Schematic diagram of thermal CVD reactor used in modeling.

mass transfer must be solved together with the equations for the gaseous and surface reactions to describe the CVD process quantitatively.

Although standard forms of the transport equations are available in a reference [5], simplified forms may be obtained based on the following assumptions. First, the bulk phase profile is in a pseudo-steady state so that the time derivative terms in the original equations are omitted. Second, Rayleigh number indicating the relative importance of the natural convection over the forced convection is small (as shown in Table 2 and discussed later), and therefore natural convection and thermal diffusion in the reactor are neglected. The final assumptions are that the flow field satisfies the continuity equation and that the flow is laminar. Based on these assumptions, the transport equations for a two-dimensional CVD process are simplified as follows.

Continuity

$$\frac{\partial}{\partial x}(\rho v_x)+\frac{\partial}{\partial y}(\rho v_y)=0 \tag{1}$$

Momentum

$$\frac{\partial}{\partial x}(\rho v_x^2)+\frac{\partial}{\partial y}(\rho v_x v_y)=-\frac{\partial P}{\partial x}+\frac{\partial}{\partial x}\left(\mu\frac{\partial v_x}{\partial x}\right)+\frac{\partial}{\partial y}\left(\mu\frac{\partial v_x}{\partial y}\right)+\rho g_x \tag{2}$$

$$\frac{\partial}{\partial x}(\rho v_x v_y)+\frac{\partial}{\partial y}(\rho v_y^2)=-\frac{\partial P}{\partial y}+\frac{\partial}{\partial x}\left(\mu\frac{\partial v_y}{\partial x}\right)+\frac{\partial}{\partial y}\left(\mu\frac{\partial v_y}{\partial y}\right)+\rho g \tag{3}$$

Energy

$$\frac{\partial}{\partial x}(\rho C_p v_x T)+\frac{\partial}{\partial y}(\rho C_p v_y T)=\frac{\partial}{\partial x}\left(\lambda\frac{\partial T}{\partial x}\right)+\frac{\partial}{\partial y}\left(\lambda\frac{\partial T}{\partial y}\right) \tag{4}$$

Mass

Table 1. Typical operating conditions in thermal CVD

Temperature	Inlet	298 K
	Wall	773 K
	Susceptor	1073 K
Inlet composition	SiH_4	0.01 (mass fraction)
	H_2	0.99 (mass fraction)
Pressure		1 Torr
Total flow rate		500 sccm
Tilted angle		7°
Reactor dimension		3×30 cm^2

Table 2. Important dimensionless variables

Re	Reynolds No.	$Dv\rho/\mu$	0.40-0.70
Pe_t	Thermal Peclet No.	Dv/α	0.30-0.80
Pe_m	Mass Peclet No.	Dv/D_i	0.30-0.50
Ra	Rayleigh No.	$\beta g C_p \rho^2 h^3 \Delta T/\lambda\mu$	0.02-0.06
Gr	Grashof No.	$\beta g \rho^2 h^3 \Delta T/\mu^2$	0.08-0.29
Ri	Richardson No.	$\beta g h \Delta T/v^2$	0.25-0.30

$$\frac{\partial}{\partial x}(\rho v_x w_i)+\frac{\partial}{\partial y}(\rho v_y w_i)=\frac{\partial}{\partial x}\left(D_i\frac{\partial w_i}{\partial x}\right)+\frac{\partial}{\partial y}\left(D_i\frac{\partial w_i}{\partial y}\right)+r_i \tag{5}$$

where ρ, μ, C_p, and λ are physical properties calculated by considering all the species in the reactor. D_i, w_i, and r_i are diffusivity, mass fraction and production rate of i component, respectively.

2. Kinetic Expressions

Very few informations are available about the reaction mechanism and kinetics of SiH_4 pyrolysis [6-9]. Although the pyrolysis reaction includes many steps and intermediate species, the following three reactions may be considered as principal steps leading to silicon deposition [10].

$$SiH_4(g) \rightarrow SiH_2+H_2 \tag{6}$$

$$SiH_2+*_s \rightarrow SiH_2(s) \tag{7}$$

$$SiH_2(s) \rightarrow Si(s)+H_2 \tag{8}$$

A literature [3] has reported presence of SiH and SiH_3, but SiH_2 is usually known as a major species contributing to the film growth [4]. Silylene (SiH_2), generated from SiH_4 dissociation, is delivered to and adsorbed on the wafer surface eventually to decompose into silicon atom and hydrogen molecule.

The rate of SiH_4 decomposition, reaction (6), is expressed by a first-order irreversible kinetics as follows.

$$r_6=k\cdot C_{SiH_4} \tag{9}$$

k is the rate constant given by Viswanthan [7].

$$k = 1.08 \times 10^{13} \exp(-49{,}600/RT) \ [s^{-1}] \quad (10)$$

where R is the gas constant in $cal \cdot mol^{-1} \cdot K^{-1}$ and T is temperature in Kelvin scale.

3. Boundary Conditions and the Film Growth Rate

Boundary conditions for the governing equations are given below.

$x = 0$

$T = T_{inlet}$ $C_{SiH_4} = C_{inlet}$ $v_x = v_{inlet}$ $v_y = 0$

$x = x_L$

$\partial\phi/\partial y = 0$ $(\phi = T, C_i, v_x)$

$y = 0$, $0 < x < x_1$ or $x_2 < x < L$

$T = T_{wall}$ $v_x = v_y = C_{SiH_2} = 0$ $\partial C_{SiH_4}/\partial y = 0$

$y = y_h$

$T = T_{wall}$ $v_x = v_y = C_{SiH_2} = 0$ $\partial C_{SiH_4}/\partial y = 0$

$y = y_{sub}$, $x_1 < x < x_2$

$T = T_{sub}$ $v_x = v_y = C_{SiH_2} = 0$ $\partial C_{SiH_4}/\partial y = 0$

The first two conditions refer to the inlet and outlet conditions of temperature, composition and velocity. Temperature of the reactor wall except for the susceptor is maintained at T_{wall}, and the susceptor at T_{sub}. Decomposition of SiH_2 by reaction (8) occurs rapidly by contact with the wall, and therefore its concentration at the wall is almost zero. Flux of SiH_4 to the wall is assumed to be zero because it is not consumed on the wall but decomposes mostly in the gas phase. Since H_2 is produced by decomposition of SiH_2, H_2 flux is the same as that of SiH_2 except that the flux directions are opposite to each other, i.e.,

$$-D_{SiH_2}\frac{\partial C_{SiH_2}}{\partial y} = D_{H_2}\frac{\partial C_{H_2}}{\partial y} \quad (11)$$

Finally, the film growth rate is obtained from the SiH_2 flux onto the wafer and expressed in microns per minute as follows.

$$G = 6.00 \cdot 10^5 \cdot \frac{M_{Si}}{\gamma} \cdot \left(D_{SiH_2} \cdot \frac{\partial C_{SiH_2}}{\partial y} \right) \quad (12)$$

M_{Si} is the atomic weight of silicon(28.09 g/g-atom), and γ is the density of silicon film(2.33 g/cm^3). Units of C_{SiH_2} and y are in $gmol/cm^3$ and cm, respectively.

NUMERICAL COMPUTATION

A generalized finite difference computer program [11] has been used to solve the coupled model equations for reaction and transport phenomena. The second order parabolic forms of the partial differential equations have been reduced to six-point, finite difference forms, and then solved with TDMA(Tri-Diagonal Matrix Algorithm) [12] by marching integration through the finite differnce grid of 27×27 points.

SIMPLE(Semi-Implicit Method for Pressure Linked Equations) [12] algorithm and upwind scheme have been adopted for correct solution and program stability. Typical computational run has required about 10 hours using a personal computer of 386-SX.

RESULTS AND DISCUSSION

1. Typical Results

The major variables in CVD processes are substrate temperature, pressure, flow rate, and inlet concentration. To find the effect of these variables on the film growth rate and uniformity, each variable has been varied by three or four times in this study. Typical ranges of these variables have been listed in Table 1, and the dimensionless variables calculated from these values are listed in Table 2.

Since Reynolds number which characterizes the flow pattern in the reactor is very small, laminar flow has been developed in the reactor. Fig. 2, which is obtained for a typical operating condition of Table 1, demonstrates that the reactant flows in a well-developed laminar pattern. Velocity arrows are closely spaced near the substrate because many grid points have been used to minimize computational errors.

According to Schlichting [13], the entrance length, L_h, of a laminar flow in a channel with height, h, is determined by the following expression.

$$L_h = 0.04 \times h \times Re,$$

where Re is Reynolds number. Since the entrance length of the model reactor in this study is 0.16 ($0.04 \times 10 \times 0.4$) cm, the flow is fully developed near the entrance. Velocity is very high near the substrate due to volume expansion resulting from the hot substrate and the silane dissociation.

Thermal and mass diffusive effects cannot be neglected in LPCVD process because the thermal and mass Peclet numbers, which measure the relative importance of convection to diffusion, are very low. Temperature distribution in the reactor is shown in Fig. 3. As the temperature rapidly increases in the vicinity of the hot susceptor, a vertical buoyancy-driven flow is possible. But since the Rayleigh, Grashof, and Richardson numbers are small, the natural convective effect may be regarded almost negligible.

Isoconcentration curves of SiH_4 and SiH_2 are drawn in Fig. 4 and Fig. 5. Since no flux of SiH_4 species to-

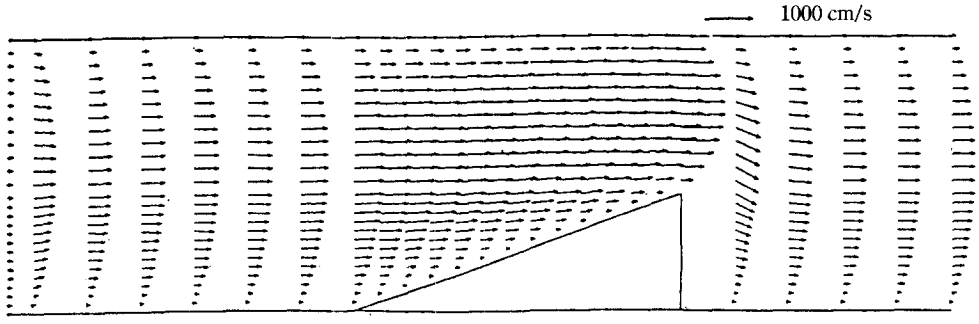

Fig. 2. Typical shape of velocity field (operating conditions in Table 1).

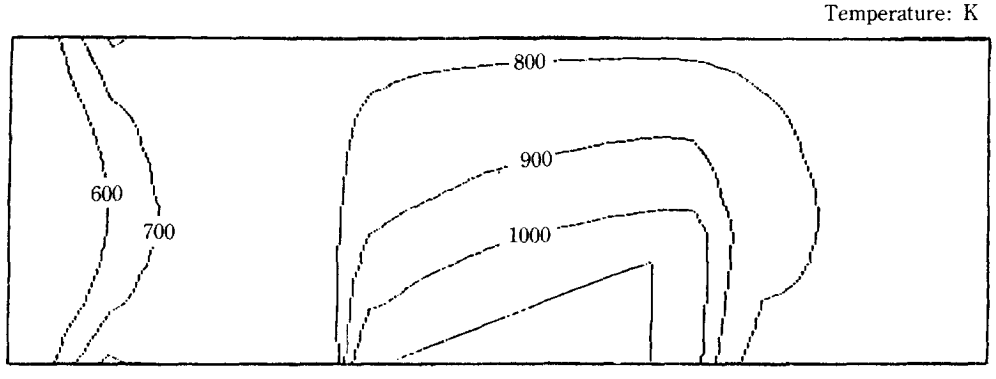

Fig. 3. Typical shape of temperature field (operating conditions in Table 1).

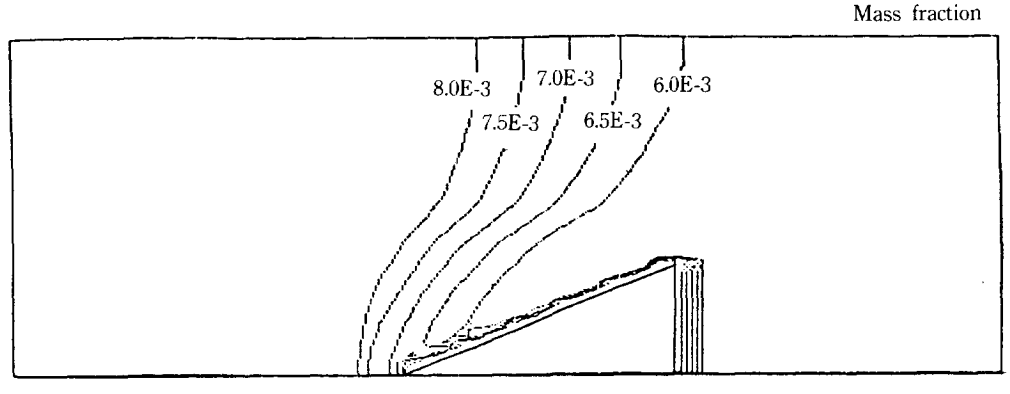

Fig. 4. Typical shape of SiH_4 concentration profile (operating conditions in Table 1).

ward the wafer or wall has been assumed in the boundary conditions, the isoconcentration curve of SiH_4 touches the wall at a right angle. Isoconcentration curves of SiH_2 which directly determine the deposition rate are parallel to the wafer surface, and therefore a uniform thickness of the deposited film is expected.

2. Effects of Flow Rate and Degree of Tilting

Variations of the Si-deposition rate along the axial reactor position is plotted in Fig. 6 for different flow rates. The film growth rate and the uniformity increase until the flow rate increases up to 300 sccm, but the growth rate decreases when the gas flows faster than 300 sccm. The result is somewhat unusual considering that the rate of mass transfer to the substrate is enhanced as the flow rate increases. But, this is due to the fact that the residence time of reactants

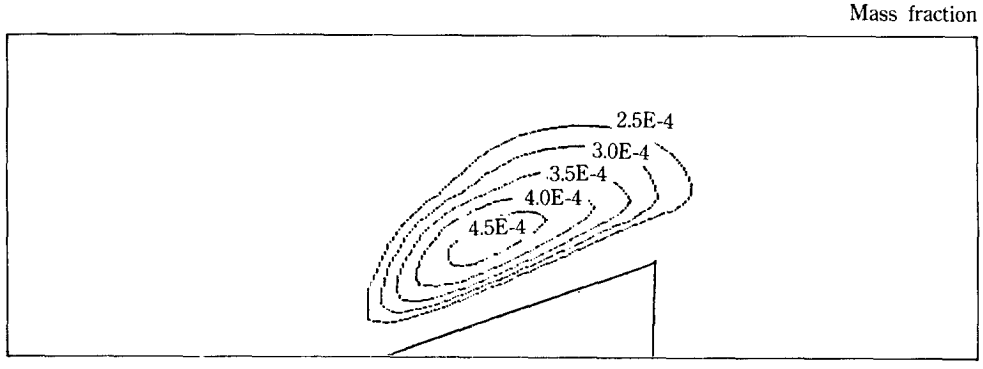

Fig. 5. Typical shape of SiH_2 concentration profile (operating conditions in Table 1).

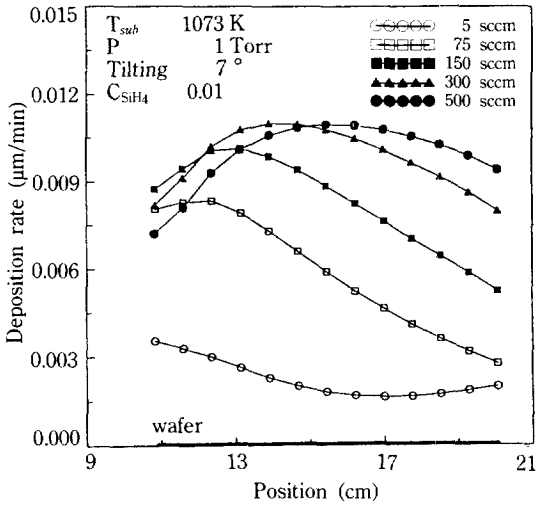

Fig. 6. Deposition rate variation with position for various flow rates in thermal CVD.

in the gas phase diminishes and therefore the amount of the intermediate species, SiH_2, decreases as the flow rate increases. In fact, Fig. 6 shows that position of the maximum film growth rate shifts towards the reactor end as the flow rate increases. Fig. 7 also shows that the film growth profile is in accordance with the SiH_2 concentration profile at different flow rates. With a small flow rate of 5 sccm, the deposition rate decreases along the axial direction and then increases slightly near the reactor end (Fig. 6). Slight increase in the deposition rate at the reactor end despite the reactant depletion along the reactor is due to high temperature of the reactant stream achieved after extended residence time above the hot substrate.

Fig. 8 shows that the deposition rate is negatively dependent on the degree of susceptor tilting. Variation in the film uniformity with flow rate and degree of tilting is also shown in Fig. 9 with normalized X-axis. Uniformity of the film is defined as follows.

$$\text{Uniformity} = \frac{G_{max} - G_{min}}{G_{max} + G_{min}} \times 100[\%],$$

where G_{max} and G_{min} are the maximum and minimum growth rates, respectively. While the uniformity is slightly improved with larger degree of tilting, it is influenced more significantly by the flow rate. As mentioned above, the large dependency of the uniformity on the flow rate agrees with the result that magnitude of the maximum SiH_2-concentration changes significantly with the flow rate.

3. Effect of Substrate Temperature

The average deposition rate increases with the substrate temperature (Fig. 10). However, above 800℃, the deposition rate decreases rapidly along the wafer position and near the end of the susceptor becomes even smaller than the rate obtained at temperatures below 800℃. Since conductive heat transfer in the axial flow direction is significant when Peclet number is small as in this study, most of the SiH_4 reactant decomposes before it reaches the substrate, particularly when the substrate temperature is very high. This results in rapid decrease of the deposition rate along the axial reactor position. Accordingly, to achieve a good film uniformity at high substrate temperatures, it is necessary to employ a high total flow rate so that the maximum decomposition rate is achieved above the substrate position in the reactor.

4. Effects of Inlet Composition and Total Pressure

Changes in the film growth rate with the inlet composition and the total pressure are shown in Fig. 11 and Fig. 12, respectively. Under the conditions of high pressure and high inlet concentration of SiH_4, the deposition rate decreases along the susceptor again because silane dissociation occurs before the substrate

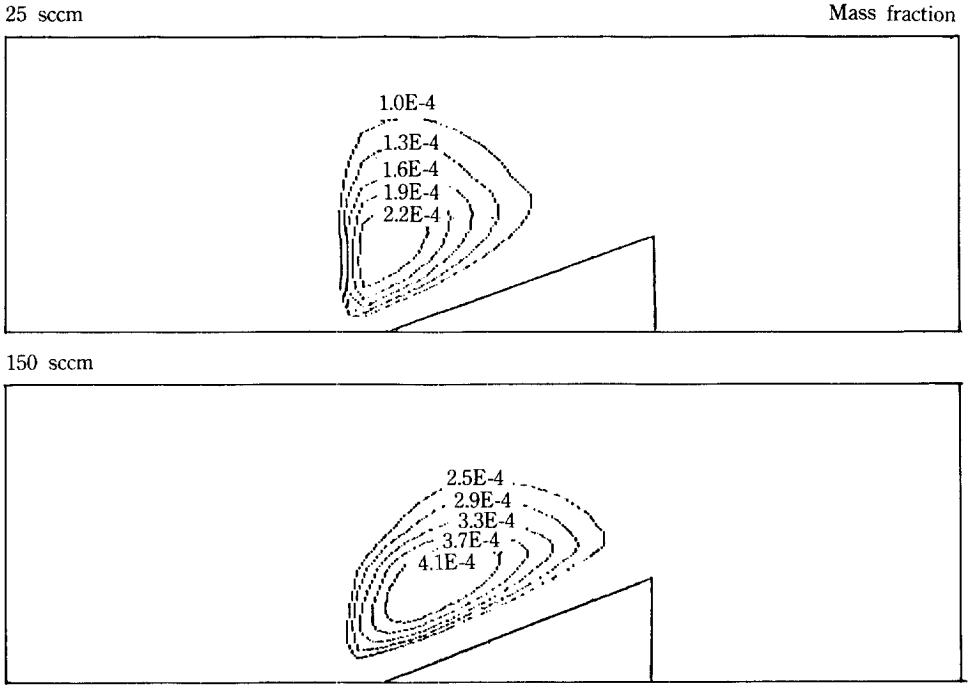

Fig. 7. SiH_2 concentration profiles for different flow rates in thermal CVD (operating conditions in Table 1).

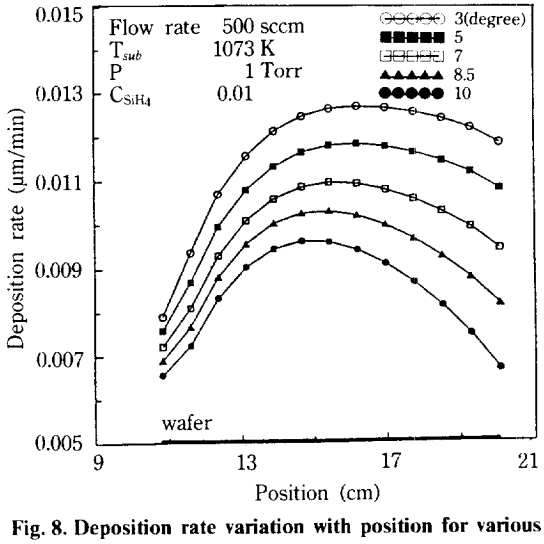

Fig. 8. Deposition rate variation with position for various degrees of substrate tilting in thermal CVD.

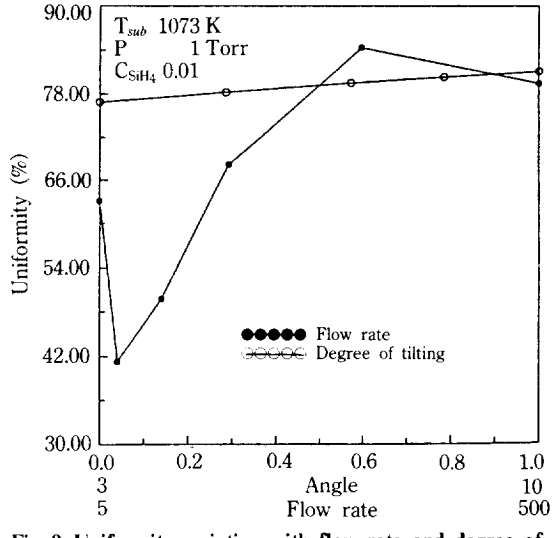

Fig. 9. Uniformity variation with flow rate and degree of tilting in thermal CVD.

region. Improved uniformity of the film thickness is obtained at lower total pressures because the mass transfer rate is enhanced at lower pressures. Fig. 12 shows that the film growth rate increases slightly at the end of the substrate, which is also due to fast mass transfer of SiH_2 species at low partial pressures.

CONCLUSIONS

Growth of silicon film by thermal decomposition of silane at relatively low temperatures in LPCVD process has been simulated by numerical solution of simplified governing equations, and the following conclu-

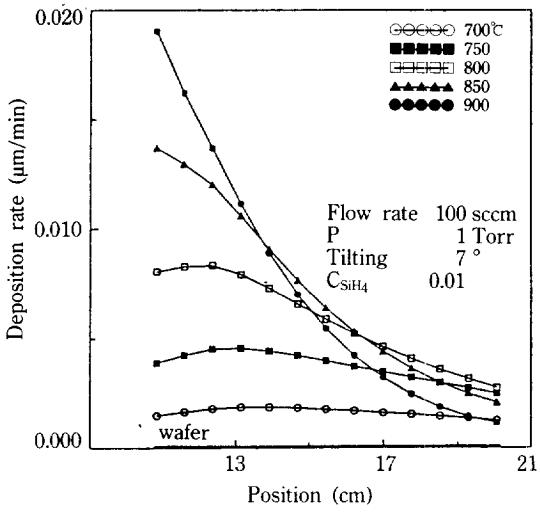

Fig. 10. Deposition rate variation with position for various substrate temperatures in thermal CVD.

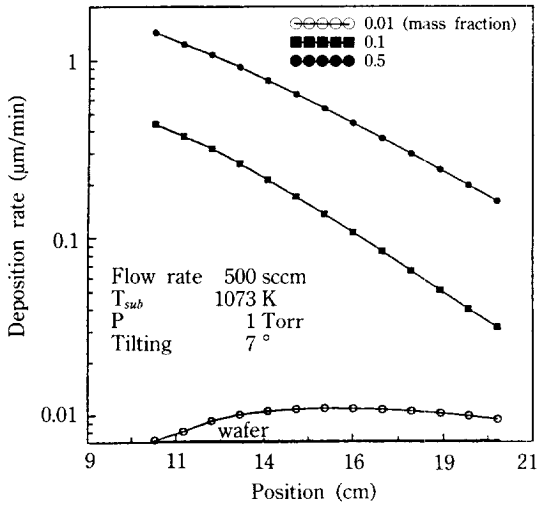

Fig. 11. Deposition rate variation with position for various inlet concentrations of SiH_4 in thermal CVD.

sions are obtained.

1. The rate of film deposition and the film uniformity increase with the reactant flow rate when the flow rate is relatively small, but decrease at higher flow rates due to the adverse effect of the reduced retention time in the reactor.

2. With a larger degree of the substrate tilting, the growth rate decreases but the film uniformity is improved.

3. When the substrate temperature and the reactant inlet concentration are high, operation with a high flow rate is advantageous for obtaining a uniform film thickness.

4. The film uniformity is improved when the pressure is low.

Under the process conditions employed in this study, the film growth rate is competitively limited either by the gas phase reaction or by the mass transfer rate.

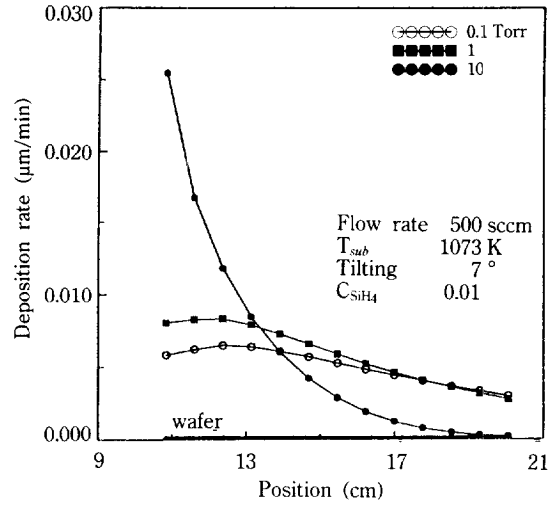

Fig. 12. Deposition rate variation with position for various total pressure in thermal CVD.

ACKNOWLEDGEMENT

This work was supported by Korea Research Foundation, 1991.

NOMENCLATURE

C_p : heat capacity
D : diffusivity
G : growth rate
G_{max}, G_{min}: maximum and minimum growth rate
g : gravity acceleration
h : reactor height
k : reaction rate constant
L_n : entrance length
M_{Si} : silicon atomic weight
R : gas constant
T_{inlet}, $T_{susceptor}$, T_{wall}: temperature of inlet, susceptor and wall
v : velocity
w : weight fraction
γ : density of silicon film
λ : heat conductivity

μ : viscosity
ρ : density

REFERENCES

1. Meyerson, B. S., Gannin, E., Smith, D. A. and Nguyen, T. N.: *J. Electrochem. Soc.*, **133**, 1232 (1986).
2. Jensen, K. F. and Graves, D. B.: *J. Electrochem. Soc.*, **130**, 1950 (1983).
3. Coltrin, M. E., Lee, R. J. and Miller, J. A.: *J. Electrochem. Soc.*, **131**, 425 (1984).
4. Coltrin, M. E., Kee, R. J. and Miller, J. A.: *J. Electrochem. Soc.*, **133**, 1206 (1986).
5. Bird, R. B., Stewart, W. E. and Light, E. N.: "Transport Phenomena", John Wiley and Sons Inc., New York (1960).
6. Viswanathan, R., Thompson, D. L. and Raff, L. M.: *J. Chem. Phys.*, **80**, 4230 (1984).
7. White, R. T., Espino-Rios, R. L., Rogers, D. S., Ring, M. A. and O'Neal, H. E.: *Int. J. Chem. Kinet.*, **17**, 1029 (1985).
8. Inoue, G. and Suzuki, M.: *Chem. Phys. Lett.*, **122**, 361 (1985).
9. Jasinski, J. M.: *J. Phys. Chem.*, **90**, 555 (1986).
10. Rhee, S. and Szekely, J.: *J. Electrochem. Soc.*, **133**, 2194 (1986).
11. Pun, W. M. and Spalding, D. B.: "A General Computer Program for Two-Dimensional Elliptic Flows", Imperial College of Science and Technology, London (1977).
12. Patanka, S. V.: "Numerical Heat Transfer and Fluid Flow", Hemisphere Pub. Corporation, Washington (1980).
13. Schlichting, H.: "Boundary Layer Theory", 6th ed., McGraw-Hill Inc., New York (1968).